Characteristics of photonic nanojets from two-layer dielectric hemisphere*

Yunyue Liu(刘昀玥)[1], Xianchao Liu(刘贤超)[1,2], Ling Li(李玲)[1], Weidong Chen(陈卫东)[1], Yan Chen(陈艳)[1], Yuerong Huang(黄跃容)[1], and Zhengwei Xie(谢征微)[1,†]

[1] College of Physics and Electronic Engineering, Sichuan Normal University, Chengdu 610101, China
[2] State Key Laboratory of Electronic Thin Films and Integrated Devices, School of Optoelectronic Information, University of Electronic Science and Technology, Chengdu 610054, China

(Received 23 May 2017; revised manuscript received 10 July 2017; published online 30 September 2017)

The properties of the photonic nanojet generated by a two-layer dielectric microsphere are studied. Simulation results indicate that this novel structure can generate a photonic nanojet outside its volume when the refractive index contrast relative to the background medium is higher than 2:1 in the condition of plane wave incidence. When the refractive index is smaller than 2, we show that an ultralong nanojet generated by the two-layer hemisphere has an extension of 28.2 wavelengths, and compared with the homogeneous dielectric hemisphere, it has superior performance in jet length and focal distance. Its dependence on the configuration and refractive index is investigated numerically. According to the simulation of the two-layer dielectric microsphere, a photonic nanojet with a full width at half maximum (FWHM) less than 1/2 wavelength is obtained and the tunable behaviors of the photonic nanojet are demonstrated by changing the reflective indices of the material or radius contrast ratio.

Keywords: photonic nanojet, hemisphere, micro-optics, subdiffraction

PACS: 42.25.Bs, 42.50.St, 78.67.–n **DOI:** 10.1088/1674-1056/26/11/114201

1. Introduction

A specific phenomenon named photonic nanojet was first numerically discovered in Ref. [1]. When a plane-wave illuminates a dielectric microsphere, a high-intensity electromagnetic beam (photonic nanojet) will appear and propagate from the shadow-side surface. A photonic nanojet is a non-evanescent propagating beam[2] with a high intensity that can significantly exceed the intensity of the incident light (I_0), and it can extend farther than the incident wavelength (λ). Moreover, photonic nanojet has a subwavelength waist and its minimum full width at half maximum (FWHM) beamwidth can be smaller than the classical diffraction limit.

A photonic nanojet can provide a high-intensity electromagnetic beam in a narrow space, so it can be used to detect nanoparticles of size well below the classical diffraction limit[3] and it is available for photolithography on the nanoscale.[4,5] Due to their superior performance, photonic nanojets have good application prospects in microscopy,[6–8] low-loss waveguide,[9,10] and ultrahigh-density optical storage.[11] Besides microspheres, researchers have designed many structures to obtain photonic nanojets, such as microdisk,[12] axicon particles,[13] hemispheric shell,[14] elliptical particles,[15] irregular particle,[16] and microparticle array.[17–19]

However, the results of the previous research show that the photonic nanojet generated from a microsphere can only exist outside of the structure under the condition of the refractive index contrast relative to the background lower than 2:1,[20] so the microsphere with $n > 2$ cannot be used in air. In this aspect, the application range of photonic nanojet would be limited. From the point of view of application, researchers expect that the photonic nanojets extend as far as possible in the propagating direction. To achieve this goal, some research about photonic nanojet has been done. Studies found that a composite particle with graded-index can lengthen the nanojet.[21–23] Later, Shen *et al.* showed that for a two-layer microsphere, the effective length of the photonic nanojet could be extended to 22λ.[24] Further study found that an extra long photonic nanojet can be generated by liquid-immersed microparticles,[25–27] but the low intensity and wide beam waist restrict its application. Besides, Liu *et al.* found that a photonic nanojet generated from a truncated dielectric microsphere is tunable through variation of the cutting thickness.[28]

Inspired by the research mentioned above, in this paper, a novel structure, i.e., a microparticle with a two-layer dielectric hemisphere configuration, is proposed. This two-layer dielectric hemisphere can combine the superiorities of multilayer structure and truncated dielectric microsphere. Comparing with the conventional microsphere, the two-layer di-

*Project supported by State Key Laboratory of Optical Technologies on Nano-Fabrication and Micro-Engineering, Institute of Optics and Electronics, Chinese Academy of Sciences; Sichuan Provincial Department of Education, China (Grant No. 16ZA0047); the State Key Laboratory of Metastable Materials Science and Technology, Yansan University, China (Grant No. 201509); and the Large Precision Instruments Open Project Foundation of Sichuan Normal University, China (Grant Nos. DJ2015-57, DJ2015-58, DJ2015-60, DJ2016-58, and DJ2016-59).

†Corresponding author. E-mail: zzwxie@aliyun.com

© 2017 Chinese Physical Society and IOP Publishing Ltd

electric hemisphere can easily focus on the outside when the refractive index contrast relative to the background medium is higher than 2:1, and generate a photonic nanojet far from its flat surface. In addition, the photonic nanojet from the novel structure has superior performance in the jet length and the focal distance compared to that from the homogeneous hemisphere. It is possible to obtain such microparticles experimentally with the development of the fabrication techniques. Thermal reflow process[29] and ion exchange technique[30,31] show the viability in future experiments.

2. Numerical model

Here we consider a dielectric composite hemisphere consisting of a core and a concentric shell with different refractive indexes. Figure 1(a) shows the schematic diagram of the two-layer dielectric hemisphere. Figure 1(b) shows the key parameters of the two-layer dielectric hemisphere, which consists of a core with the radius $R_c = 1.5$ μm and a shell with the radius $R_s = 3$ μm. Their reflective indices are n_c and n_s, respectively. The surface of the hemisphere overlaps with the x–y plane and its center is at the origin of the coordinate system. The whole structure is placed in the air. Light source, an y-polarized plane wave with wavelength $\lambda = 400$ nm and unit intensity, propagates along the z-direction and impinges on the two-layer dielectric hemisphere from left.

We use four key parameters to characterize the photonic nanojet quantitatively: the peak intensity I_P, the focal distance f from the shadow side surface to the focal point, the effective length L, which is from the focal point to the point where the intensity drops to $1/e$ of I_P, the jet length D, which is from the shadow side surface to the point where the intensity is $2I_0$ (intensity of the incident light), and the FWHM w of the focal point in the y-direction. In this paper, we choose the wavelength as the unit of the parameters.

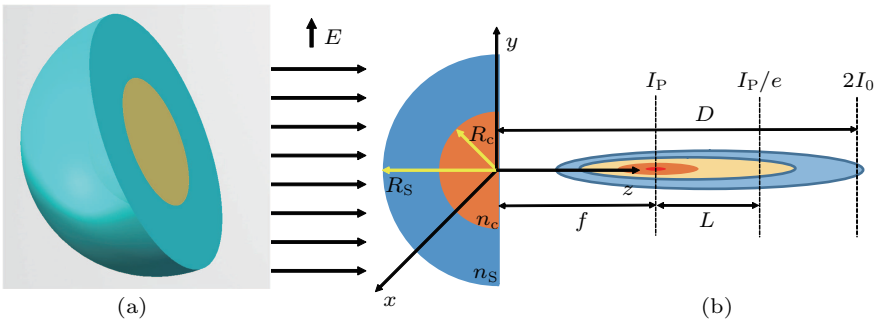


Fig. 1. (color online) (a) Schematic diagram of two-layer dielectric hemisphere. (b) The two-layer dielectric hemisphere illuminated by a plane wave and key parameters of the photonic nanojet.

3. Result and discussion

We use CST simulation software to study theoretically the characteristics of photonic nanojets, which are generated at the shadow side surface of the two-layer dielectric hemisphere illuminated by a plane wave. Figure 2(a) shows the situation of photonic nanojet formation from a conventional microsphere in air with $R = 3$ μm and $n = 2$ (silicon nitride[24]). It is clear that the microsphere focuses the incident light mostly inside its volume. In order to focus on the outside, we consider a two-layer dielectric hemisphere with $R_c = 1.5$ μm, $n_c = 2.0$ and $R_s = 3$ μm, $n_s = 2.8$ (Brookite) as an example. Figure 2(b) is the optical field intensity distribution in the y–z plane of the two-layer hemisphere. The results show that the two-layer dielectric hemisphere can focus the incident beam away from the surface. So we can easily obtain photonic nanojets outside a two-layer dielectric hemisphere when the refractive index contrast relative to the background medium is higher than 2:1. That is to say, we can fabricate particles by some high refractive index materials such as barium titanate,[14] doped semiconductor,[24] diamond,[32] and potassium tantalate.[33]

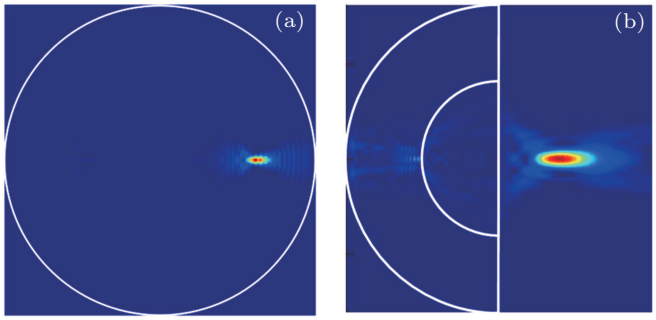


Fig. 2. (color online) Normalized intensity distributions of photonic nanojets generated from (a) a homogeneous dielectric microsphere with $R = 3$ μm, $n = 2.0$ and (b) a two-layer dielectric hemisphere with $R_s = 3$ μm, $n_s = 2.8$ and $R_c = 1.5$ μm, $n_c = 2.0$.

Although truncated microspheres such as hemispheres can also achieve the goal mentioned above, the photonic nanojet generated by the two-layer dielectric hemisphere has superior performance in jet length and focal distance, especially for low refractive index materials. The simulation results show that the photonic nanojet generated from the two-layer dielectric hemisphere has a good performance when the refractive index of the material is less than two. The two-layer dielectric hemisphere composed of conventional optical materials also

has the capacity to generate a high quality photonic nanojet. Figures 3(a) and 3(b) show the simulation results of a hemisphere placed in air with different structures. From Figs. 3(a) and 3(b), we find that the photonic nanojet generated from the two-layer dielectric hemisphere has a jet length D of 28.2λ, which is almost three times as long as that of the homogeneous dielectric hemisphere. The FWHM increases compared with the homogeneous dielectric hemisphere while the focal distance increases by 5.75λ (f increases from 2.84λ to 8.59λ). Although the intensity of the focal point decreases to 36% compared with the homogeneous dielectric hemisphere, it is still a high intensity. From the above, the two-layer dielectric hemisphere can focus the incident beam outside its volume when the refractive index contrast relative to the background medium is higher than 2:1, such a capability may provide more choice of material to fabricate the microparticles. Moreover, the ultralong jet length will make the nanojet more viable in rough surfaces of samples and far-field applications.

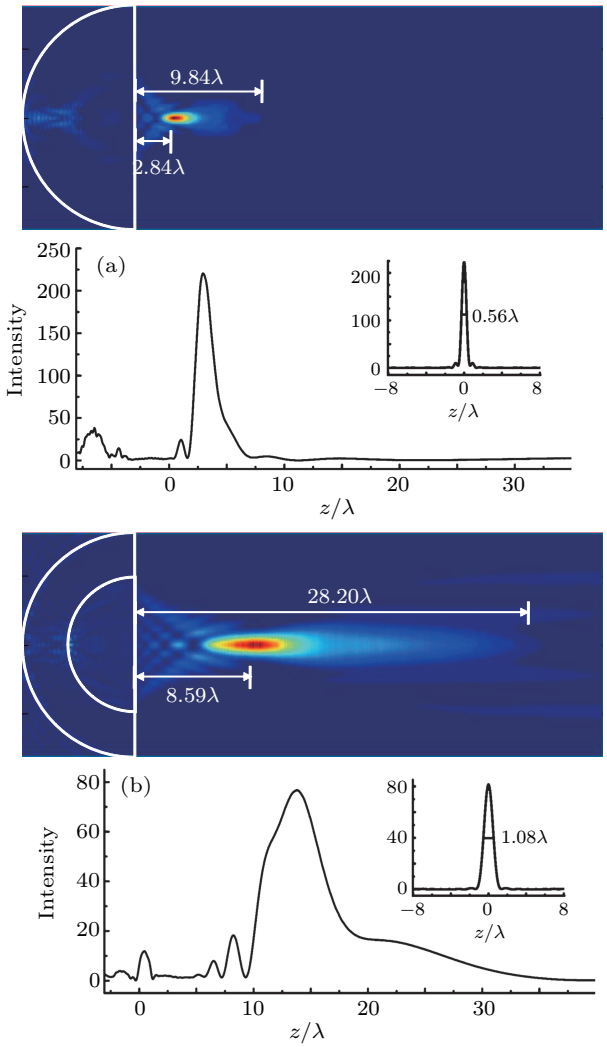


Fig. 3. (color online) Normalized intensity distributions of photonic nanojets generated from (a) a single dielectric hemisphere with $R = 3$ μm, $n = 1.8$ and (b) a two-layer dielectric hemisphere with $R_s = 3$ μm, $n_s = 1.8$ and $R_c = 1.8$ μm, $n_c = 1.5$. The lower panel plots the intensity profile along the z direction, and the transverse profile at the focal point is also shown in the inset.

The light distribution through the two-layer hemisphere at different incident wavelengths from 400 nm to 1000 nm is investigated. Figures 4(a)–4(d) show the normalized intensity distributions of photonic nanojets at different incident wavelengths through a two-layer dielectric hemisphere ($R_s = 3$ μm, $n_s = 1.8$, and $R_c = 1.5$ μm, $n_c = 1.5$). As the incident wavelength increases, the focal distance f decreases from 3.21 μm to 1.72 μm. The light through the core region tends to scatter from optically denser medium to optically thinner medium, so that emergent light focuses far away from the surface. The longer the wavelength of the incident light is, the weaker the refraction effect is, besides, less light enters the core region, therefore, the focal distance f decreases with increasing incident wavelength. At the same time, as the incident wavelength increases, the peak intensity I_P decreases while the FWHM increases. The two-layer hemisphere illuminated by a plane-wave with a wavelength of 400 nm can generate a photonic nanojet with better performance. So we choose 400 nm as the incident wavelength in the simulation below.

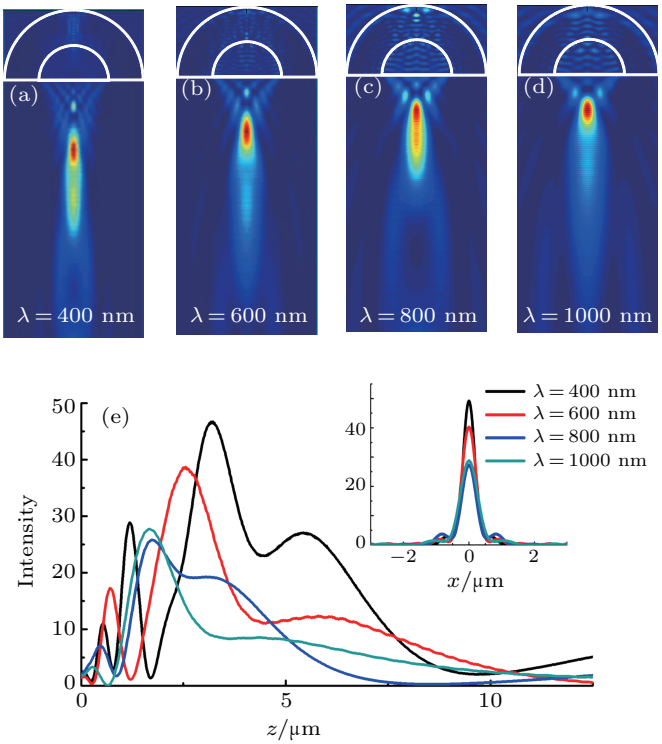


Fig. 4. (color online) (a)–(d) Normalized intensity distributions of photonic nanojets at different incident wavelengths through a two-layer dielectric hemisphere with $R_s = 3$ μm, $n_s = 1.8$, and $R_c = 1.5$ μm, $n_c = 1.5$. (e) The intensity profiles along the z direction of photonic nanojets at different incident wavelengths, and the transverse profiles at the focal point are also shown in the inset.

Considering structural differences from production processes of microparticles, the effect of the radius contrast ratio on photonic nanojet is studied. Figures 5(a)–5(j) show that the photonic nanojets generated from two-layer hemispheres in air with different radius contrast ratios. The plane wave with wavelength $\lambda = 400$ nm and unit intensity impinges on

the two-layer dielectric hemisphere from the top. The n_s, n_c, and R_s are kept at 1.8, 1.5, and 3 μm respectively, while the radius contrast ratio is varied from 10:0 to 10:9. It is obvious that the radius contrast ratio plays an important role in determining the properties of the photonic nanojet. From the intensity distribution, the key parameters of the photonic nanojet vary a lot when changing the value of $R_s : R_c$. We obtain an ultralong nanojet with jet length D of 11.28 μm ($\sim 28.20\lambda$) when $R_s : R_c = 10 : 6$. The simulation results show that we can obtain an ultralong photonic nanojet by adjusting the radius contrast ratio. Even with a radius contrast ratio lower than 10:7, the two-layer hemisphere could focus the incident light to a single point rather than a series of disconnected points in Ref. [14].

In Figs. 5(a)–5(f), as the radius contrast ratio decreases, the focal distance f and the effective length L become longer while the intensity becomes weaker. In contrast, in Figs. 5(g)–5(j), as the radius contrast ratio decreases, f and L become shorter while the intensity becomes stronger. The change of the structure is the reason why the key parameters do not vary monotonously. Figure 5(a) shows that in homogeneous dielectric hemisphere, the light through the core region is focused with a lesser angle against the axis compared to the light transmitting through the margin, due to the difference of the incident angle at the convex side of the hemisphere.[13] In fact, more than one focal point can exist along the propagation direction. By changing the core material from optically denser medium to optically thinner medium, the light through the core region tends to scatter, so that emergent light focuses far away from the surface. When R_c increases, more light transmitting through the core leads to a longer focal distance f. As the radius contrast ratio decreases, the light through the core and the margin tend to get close with considerable intensity, finally merging into a single focal point in the intensity distribution and form a photonic nanojet with a long jet length. However, as the contrast ratio decreases continuously, less light transmitting through the margin and light through the core is almost dominant, so f and L become shorter. Photonic nanojets generated from hemispheres with different radius contrast ratios from 10:5 to 10:9 can be used in practical applications.

The refractive index of the materials has an influence on the intensity distribution. Figures 6(a) and 6(b) show the focal distance f, the FWHM w, the intensity I_P, and the effective length L of the photonic nanojet when the reflective index (n_s) of the shell is varied from 1.4 to 1.8. In Fig. 7, as n_s increases, the focal distance f, the FWHM w, and the peak intensity I_P decrease. Figures 7(a) and 7(b) show the simulation outcome of two-layer dielectric hemispheres with different reflective indices (n_c) of the core material. It can be seen that the peak intensity I_P increases with the reflective index increasing from 1.3 to 1.7, while the effective length L, the focal distance f, and the FWHM w are up to their maxima, respectively. In the two cases mentioned above, all parameters change a lot with increasing reflective indices of the materials. It is worth noting that the focal distance f and the FWHM w have the same trend. Moreover, the minimum of FWHM w is 167.8 nm ($n_s = 1.6$, $n_c = 1.3$), which is smaller than the classical diffraction limit $\lambda/2$. That is to say, the photonic nanojet generated by the two-layer dielectric hemisphere can be tunable by changing the reflective indices of the materials.

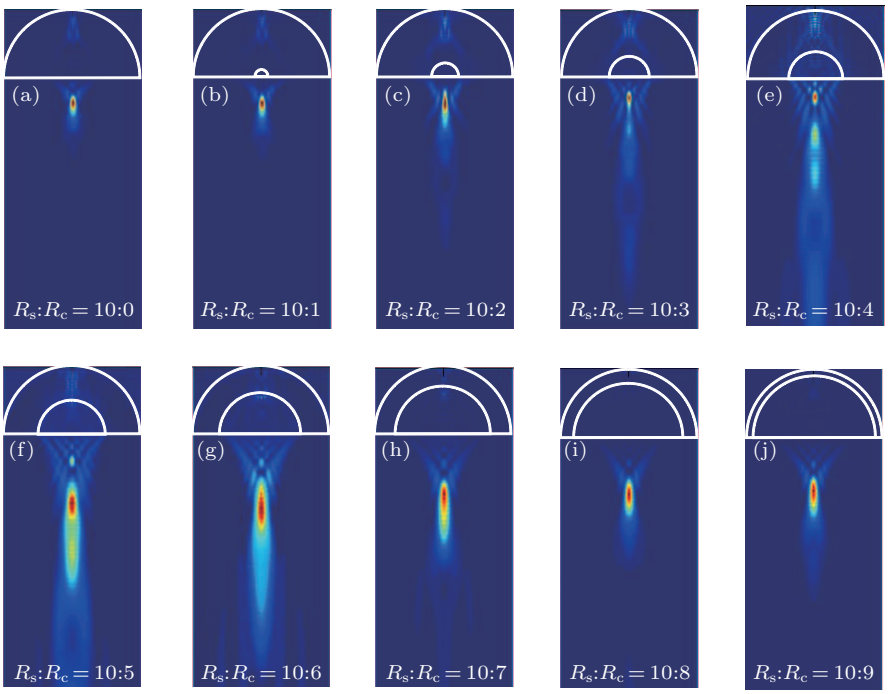


Fig. 5. (color online) Normalized intensity distributions of photonic nanojets generated from hemispheres ($R_s = 3$ μm, $n_s = 1.8$, $n_c = 1.5$) with (a)–(j) different radius contrast ratios.

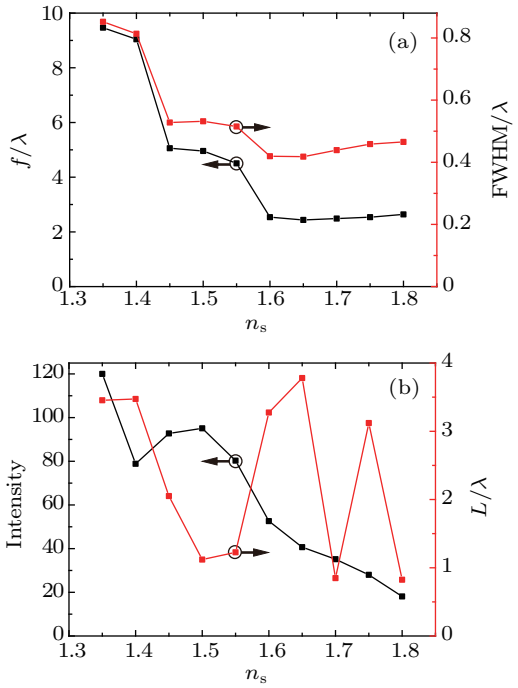


Fig. 6. (color online) Four key parameters of photonic nanojet as a function of the shell refractive index (n_s) for the two-layer dielectric hemisphere with $R_s = 3$ μm and $R_c = 1.5$ μm, $n_c = 1.3$. (a) Focal distance f and FWHM w as a function of n_s. (b) Peak intensity I_P and effective length L as a function of n_s.

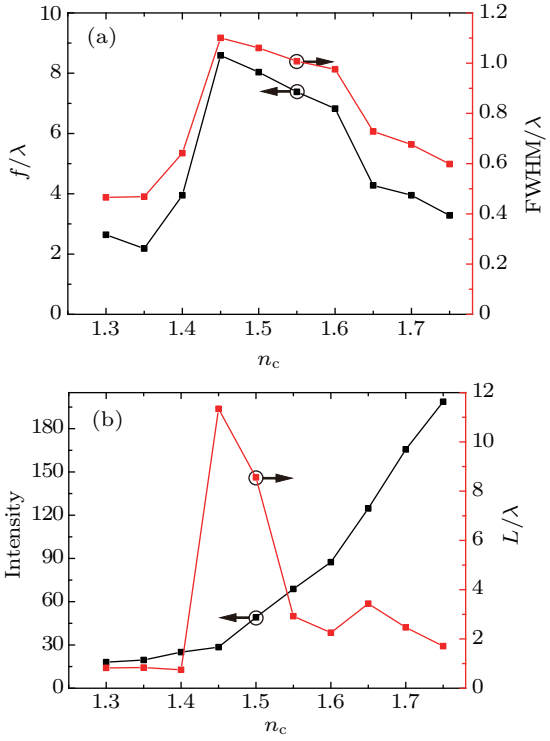


Fig. 7. (color online) Four key parameters of photonic nanojet as a function of the core refractive index (n_c) for the two-layer dielectric hemisphere with $R_s = 3$ μm, $n_s = 1.8$, and $R_c = 1.5$ μm. (a) Focal distance f and FWHM w as a function of n_c. (b) Peak intensity I_P and effective length L as a function of n_c.

We notice that the effective length L becomes complex in both cases. We choose Fig. 7 (change the material of the core when $n_s = 1.8$) as an example. A small value of n_c means a small value of n_c/n_s, which leads to a small critical angle, and the internal reflection between the core and the shell dominates while less light transmits through the core. So the low n_c in this case causes low values of I_P, f, and L. As n_c increases, the critical angle increases gradually and more light passes through the periphery of the core, so the focal distance f and the effective length L increase accordingly, then the focal point tends to be close. When the two adjacent points with considerable intensity are close enough, they may be considered as one, so the effective length L can be extra long at the moment. As n_c continuously increases, the internal reflection on the boundary between the core and air dominates, and the core tends to focus the light more efficiently, resulting in a shorter effective length L. However, the increase of n_s affects not only the light through the core, but also on the light through the margin, so the effective length L in Fig. 6(b) become more complex.

In addition, we use a parameter called figure of merit[21] Q to characterize the photonic nanojet. Kong *et al.* defined the figure of merit Q as $(I_P \times L)/w$. Figures 8(a)–8(d) show the L, w, I_P, and Q as a function of the refractive indexes of the shell (n_s) and core (n_c), respectively. Figure 8(a) shows that we can obtain a photonic nanojet with $L = 11.35\lambda$ ($n_s = 1.8$ and $n_c = 1.45$), and it is clear that the effective length L of the photonic nanojets can be ultralong when n_s is slightly larger than n_c. FWHMs of most photonic nanojets in the simulations are below the incident wavelengths, and lower FWHMs, which are below a half of the incident wavelength, are obtained when n_s is much higher than n_c. However, the peak intensity I_P weakens when $n_s < n_c$ because of the internal reflection between the shell and the core, and the maximum I_P ($n_s = 1.55$ and $n_c = 1.75$) is 17.5 times as high as the minimum I_P ($n_s = 1.8$ and $n_c = 1.3$). The distribution of I_P directly affects the distribution of Q. Figure 8(d) shows that the photonic nanojets with long effective length L (when $n_s > n_c$) have lower Q because of the lower I_P, however, it does not mean that the quality of those photonic nanojets is poor. Here, we choose two examples to explain. Figures 8(e) and 8(f) show the normalized intensity distributions of photonic nanojets with the lower figure of merit ($Q = 200$) and the higher figure of merit ($Q = 1093$), respectively. Obviously, the photonic nanojet with lower Q in Fig. 8(e) is more practicable in reality than the two disconnected focal points with higher Q. It is shown that photonic nanojets with high quality can be generated when $n_s > n_c$, and we can change materials to optimize the parameters of the photonic nanojets.

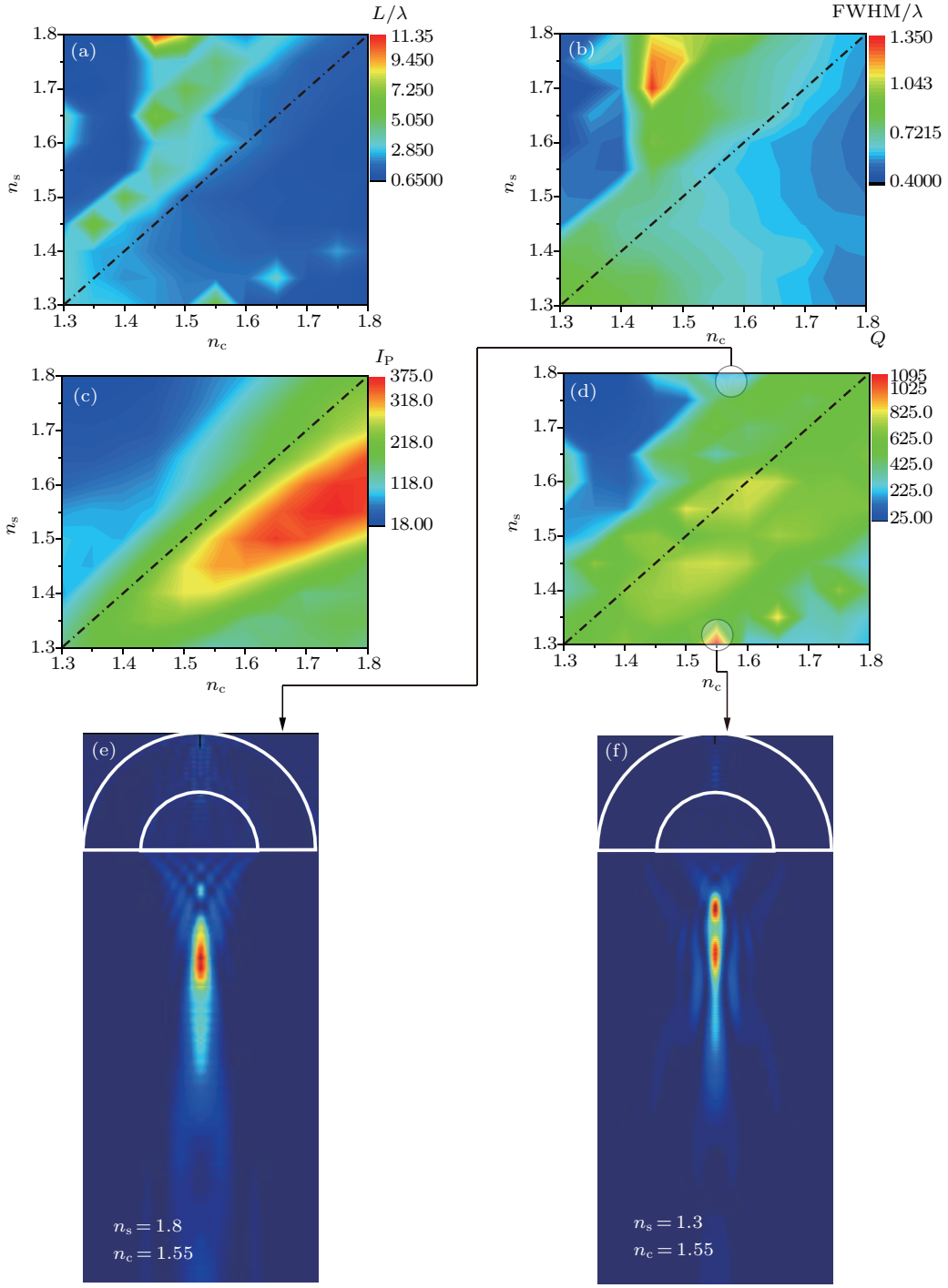


Fig. 8. (color online) (a) The effective length L, (b) FWHM w, (c) intensity I_P, and (d) figure of merit Q as a function of the refractive indexes of the shell (n_s) and core (n_c). In each illustration, the part above on the dotted line represents the situations when $n_s > n_c$. The normalized intensity distributions of photonic nanojets generated from hemispheres with (e) $n_s = 1.8$, $n_c = 1.55$, and (f) $n_s = 1.3$, $n_c = 1.55$.

4. Conclusion

This paper introduces a two-layer dielectric hemisphere to realize a photonic nanojet far away from its surface. This configuration can focus the incident beam outside its volume when the refractive index contrast relative to the background medium is higher than 2:1. Compared with the homogeneous dielectric hemisphere in the same condition, the focal distance increases by 18.36λ with a focal distance f of 8.59λ.

Moreover, the calculation results show that the effect of radius contrast ratio and refractive index of material on properties of the photonic nanojet is obvious. We obtain an ultra-long nanojet with jet length D of 11.28 μm ($\sim 28.20\lambda$) when $R_s : R_c = 10 : 6$. In our simulation calculations, the smallest FWHM w is 167.8 nm ($n_s = 1.6$, $n_c = 1.3$), which is smaller than the classical diffraction limit $\lambda/2$. In such a case, the photonic nanojet with high Q combines the merits of both high spatial localization and high peak intensity, and with the longer D brings a convenience when working in a long distance. The

photonic nanojet generated by the two-layer dielectric hemisphere is tunable by changing the reflective indices of the materials or the radius contrast ratio. We believe this study will be helpful in fields of nano-optics.

References

[1] Chen Z, Taflove A and Backman V 2004 *Opt. Express* **12** 1214
[2] Lin L, Wei G, Yinzhou Y, Seoungjun L and Tao W 2013 *Light: Sci. Appl.* **2** e104
[3] Li X, Chen Z, Taflove A and Backman V 2005 *Opt. Express.* **13** 526
[4] Mcleod E and Arnold C B 2008 *Nat. Nanotech.* **3** 413
[5] Liu X, Li X, Li L, Chen W and Luo X 2015 *Opt. Express* **23** 30136
[6] Ye R, Ye Y H, Ma H F, Cao L, Ma J, Wyrowski F, Shi R and Zhang J Y 2014 *Sci. Rep.* **4** 3769
[7] Yang H, Moullan N, Auwerx J and Gijs M A M 2014 *Small* **10** 1712
[8] Lee J Y, Hong B H, Kim W Y, Min S K, Kim Y, Jouravlev M V, Bose R, Kim K S, Hwang I C, Kaufman L J, Wong C W, Kim P and Kim K S 2009 *Nature* **460** 498
[9] Darafsheh A, Mojaverian N, Limberopoulos N I, Allen K W, Lupu A and Astratov V N 2013 *Opt. Lett.* **38** 4208
[10] Liu C Y and Li C C 2016 *Optik* **127** 267
[11] Kong S C, Sahakian A, Taflove A and Backman V 2008 *Opt. Express* **16** 13713
[12] Ju D, Pei H, Jiang Y and Sun X 2013 *Appl. Phys. Lett.* **102** 171109
[13] Geints Y E, Panina E K and Zemlyanov A A 2015 21*st International Symposium on Atmospheric and Ocean Optics: Atmospheric Physics*, November 1 2015, Tomsk, Russia, p. 96800X-1
[14] Zhu H Y, Chen Z C, Chong C T and Hong M H 2015 *Opt. Express* **23** 6626
[15] Jalali T and Erni D 2014 *J. Mod. Opt.* **61** 1069
[16] Nayak C, Mukharjee S and Saha A 2016 *Optik* **127** 8836
[17] Wang T, Kuang C, Hao X and Liu X 2011 *J. Opt.* **13** 035702
[18] Yang H, Cornaglia M and Gijs M A M 2015 *Nano Lett.* **15** 1730
[19] Xu C, Zhang S, Shao J, Lu B R, Mehfuz R, Drakeley S, Huang F and Chen Y 2016 *Nanotechnology* **27** 165302
[20] Heifetz A, Kong S C, Sahakian A V, Taflove A and Backman V 2009 *J. Comput. Theor. Nanosci.* **6** 1979
[21] Kong S C, Taflove A and Backman V 2009 *Opt. Express* **17** 3722
[22] Liu C Y 2013 *PIER. Lett.* **37** 153
[23] Geints Y E, Zemlyanov A A and Panina E K 2011 *Quantum Electron.* **41** 520
[24] Shen Y, Wang L V and Shen J T 2014 *Opt. Lett.* **39** 4120
[25] Gu G, Zhou R, Chen Z, Xu H, Cai G, Cai Z and Hong M 2015 *Opt. Lett.* **40** 625
[26] Wang Z B, Guo W, Pena A, Whitehead D J, Luk'yanchuk B S, Li L, Liu Z, Zhou Y and Hong M H 2008 *Opt. Express* **16** 19706
[27] Wu P, Li J, Wei K and Yue W 2015 *Appl. Phys. Express* **8** 112001
[28] Liu C Y 2014 *Physica E* **64** 23
[29] Hsin-Ta H, Vinna L, Jo-Lan H and Guo-Dung J S 2011 *Opt. Commun.* **284** 5225
[30] Masahiro O, Kenichi I, Takeshi S, Noboru Y and Kouichi N 1981 *Jpn. J. Appl. Phys.* **20** L296
[31] Ottevaere H, Cox R, Herzig H P, Miyashita T, Naessens K, Taghizadeh M, VölkelR, Woo H J and Thienpont H 2006 *J. Opt. A Pure. Appl. Opt.* **8** 407
[32] Masataka S, Kimihiro S, Takao K, Ariyoshi N, Motohiro F, Minoru T, Masanobu Y, Thomas J S, Bart M V O, Herman P G, Paul A C K, Evert P H, Wim H M N, Gert J P and Paul G M S 2006 *Jpn. J. Appl. Phys.* **45** 1311
[33] Kazuo F and Masahiro S 2007 *NTT. Tech.* **5** 1